DE GRUYTER Holzforschung
Wood Research & Technology

Natural cork and its agglomerates as substitutes for high-density expanded-polystyrene foams in sandwich cores

Journal:	*Holzforschung - International Journal of the Biology, Chemistry, Physics and Technology of Wood*
Manuscript ID	HOLZ.2021.0004.R2
Manuscript Type:	Original Article
Date Submitted by the Author:	n/a
Complete List of Authors:	Miralbes, Ramon; University of Zaragoza, Ranz, David; University of Zaragoza Gomez, Jose Antonio; University of Zaragoza Zouzias, Dimitris; Katholieke Universiteit Leuven,
Section/Category:	Technology
Keywords:	cork, sandwich-structured composite, tensile, natural core, shear, traction

Reviewer: 1

A thorough revision of the manuscript was requested by reviewers.

However the manuscript is still confusing regarding Materials and methods which includes a lot of discussions with regard to different ways of testing. This should preferably be discussed and commented in the section results and discussion.

- It has been modified

The presentation of the experimental procedure is also a combination of trivial parameters and more specialized. It would be good to make this presentation more addressing the lesser used constant not presenting school-book constants. A good way could be to have figures similar to figure 2 for the other testing cases as Supplementary figures.

- It has been provided.

Material presented as "additional" Should be given as Supplementary figures.

- It has been modified

Figures 3, 4, 6, 7 are still not readable the text on axis most be made larger and readable.

- Text has been made lager and readable and it has been improved the general quality of the images.

An English revision must be performed. Especially the added material is not provided in acceptable English.

- It has been checked and, afterwards performed using the Elsevier Language Service. It has been attached the certificate.

The manuscript still at some positions referral's to figures numbered according to the old submission and no longer existing.

- It has been checked and modified

The extensive tables are not very much commented on. It could serve the reader more if key-parameters were presented as figures and the tables were supplied as supplementary material.

- Tables 2 to 4 has been provided has supplementary material. It has been added some figures with the most important information of the table

Natural cork and its agglomerates as substitutes for high-density expanded-polystyrene foams in sandwich cores

R. Miralbes[a]*, D. Ranz[a], J.A. Gomez[a], D. Zouzias[b]

[a]*Department of Design and Manufacturing, University of Zaragoza, Zaragoza, Spain*

[b]*Department of Design and Manufacturing of the Catholic University of Leuven, Leuven, Belgium.*

Natural cork and its agglomerates as substitutes for high-density expanded-polystyrene foams in sandwich cores

Natural cork and its agglomerates are renewable materials that could be effective substitutes for non-renewable foams, such as expanded polystyrene (EPS), in the cores of sandwich materials. Although many existing studies have analysed the behaviour of different cork agglomerates under tensile, compression, or shear loads, no studies to date have simultaneously analysed the behaviour of multiple cork materials under all these loads. Therefore, in this study, the behaviour of natural cork and five cork agglomerates were analysed under tensile, compression, and shear loads, and the mechanical and specific properties and the shape of the stress–strain curves were compared with those obtained for five EPS counterparts to analyse the relationship between the mechanical behaviour of the core and the main failure modes of the sandwich. Although EPS exhibited higher specific properties, natural cork exhibited higher mechanical properties under all the loads. The agglomerates all exhibited lower mechanical properties except for shear strain. Additionally, because no specific standards were available for testing cork products, slightly modified standards for testing other materials were adopted.

Keywords: cork, sandwich-structured composite, tensile, natural core, shear, traction, compression

1. Introduction

Producing more environmentally friendly products is essential for reducing carbon footprints. Therefore, it is imperative to substitute non-renewable petroleum-based materials with renewable ones. In addition, sandwich-structured composites composed of a low-density thick core and two stiff and rigid face plates must be bio-degradable and recyclable after their useful life. Recently, Bach et al. (2017) have addressed these issues and developed a completely bio-degradable and renewable sandwich-structured composite using hardwood face skins, a natural glue, and a mushroom foam core, which provided higher impact and bending properties. Sadeghian et al. (2018) compared the

use of natural and synthetic materials (flax and glass fibres, respectively) for the face plates and honeycomb-structured white cork agglomerate (density unspecified) for the core and found that although the natural materials were comparable to the synthetic ones, the mechanical properties (especially the through-thickness and core-shear strengths) had to be improved.

Notably, balsa wood is a renewable material, which has been extensively used in sandwich-structured composites. Owing to the high mechanical strength, stiffness, and low weight of balsa wood, such materials provide outstanding specific mechanical properties. Therefore, balsa wood core, obtained from Core Lite Composites, was used in the study, and its properties are listed in the tables for comparison with those of expanded polystyrene foam (EPS) and cork products.

Additionally, Le Duigou et al. (2011) compared sandwiched bio-materials (made of poly-L-lactic acid/flax mat bio-composite laminate for face plates and balsa cores) with reference materials (glass-mat-reinforced polyester composite for face plates and balsa cores) and found that, despite the environmental attractiveness of bio-composites and sandwiched bio-materials, they are heavier, thereby penalising them in applications where lightweight materials are essential.

Zaini et al. (2020) reviewed the application of natural fibre composites to core structures and their broader application potential including the substitution of cork agglomerates for some foams. The authors focused on the substitution of EPS cores with cork and its agglomerates owing to their similar densities. Cork and its agglomerates are renewable materials obtained from *Quercus suber*, an oak tree mainly found on the Iberian Peninsula. Harvesting cork is environmentally friendly because the bark is stripped, leaving the tree alive for future use. Because cork is only harvested

every nine years, the bark can grow until reaching an acceptable thickness.

Silva et al. (2005) and Díaz-Parralejo et al. (2014) conducted an exhaustive analysis of the internal structure and properties of cork and determined the most important factors were the low density, near-impermeability to liquids and gases, high friction coefficient, thermal isolation properties, near-zero Poisson coefficient, flexibility, compressibility, mechanical strength, inertness and chemical resistance, resistance to biological corrosion, flame retardance, ease of machining, acoustic and anti-vibration properties, high elasticity, and the ability to recover its initial form after high-compression deformation. However, despite these excellent properties, the traditional applications of cork are mainly wine stoppers, pin boards, floorings, and roughing. Recently, however, new applications for cork have included thermal isolators in buildings, aggregates to lighten concrete colour, seals, helmet liners, etc.

Cork and its agglomerates could be applied to the core of sandwich materials, which has been extensively studied in recent years. Reis and Silva (2009) studied the mechanical properties of 3 cork-agglomerate cores applied to carbon/epoxy faces under 3-point bending and shear tests and compared them with the corresponding mechanical properties of Euro-Composite® aerospace (ECA)-grade honeycomb and ROHACELL® cores. The authors found that for the cork-sandwich core, the shear properties and maximum load measured under the 3-point bending test were much lower.

Najafi et al. (2020) analysed the use of cork agglomerates in maritime applications wherein moisture damage, which causes mechanical degradation, was identified as one of the main drawbacks and found that cork cores provided excellent resistance against environmental moisture.

Sadeghian et al. (2018) compared polypropylene honeycomb and cork cores under

flexure loads and found that cork had a 44% lower shear modulus and a 22% lower shear strength than honeycomb.

Other researchers have developed eco-friendly composites using cork cores and wooden panels. For example, Lakreb et al. (2015) studied cork agglomerate cores with different thicknesses and wooden panels for the skins and inside the core. The sandwich-structured composites were analysed under perpendicular tensile and compression, pure compression, pure compression with buckling, shear, and 3- and 4-point bending tests. The main findings were that under perpendicular tensile loads, failure occurred inside the cork core. In the 3- and 4-point bending tests, the failure was caused by core-shear failure. In the shear test, the core interior failed when the load exceeded the ultimate shear strength of the cork core. In the transversal compression test, failure was the result of a combination of bending and blistering. Failure occurred by blistering with the appearance of cracks or shear.

Although many previous studies have investigated sandwich-structured composites by focusing on the core and skin, few have detailed the mechanical behaviour of cork materials and among them, most have mainly focused on compression loads. For example, Jardin et al. (2015) studied 5 agglomerate corks and 4 expanded agglomerate corks exhibiting different grain sizes and densities and prepared using different binders as substitutes for EPS in helmet liners. The materials were tested under quasi-static compression loads. The authors concluded that the heterogeneous behaviour of the materials depended on the manufacturing process, glue used, and grain size. Consequently, the mechanical behaviour of the materials could be tailored by varying the parameters. Similarly, Fernandes et al. (2015) compared different cork agglomerates and expanded corks with different EPSs and expanded polypropylene (EPP) foams under quasi-static compression and dynamic loads from a drop tower. The authors

found that the synthetic materials exhibited higher plateau stresses and Young's moduli, allowing the materials to absorb more energy. However, the natural materials exhibited higher endurance under multiple impacts.

Laura and Rossit (2001) found that the main failure modes of sandwich structures were face-sheet failure, dimpling, and wrinkling; core-shear failure, buckling, and crushing; global buckling; and skin separation. Triantafillou and Gibson (1987) found that of these failure modes, face-sheet wrinkling, core-shear failure and buckling, core crushing, and skin separation were highly affected by the core mechanical properties. Wadsworth et al. (2009) found that face-sheet wrinkling was a complex local failure mode in which—depending on the compression, traction, and shear properties of the core and skin—short-wavelength buckling appeared on the face sheet. Other teams found that core-shear failure (Carlsson et al., 1991) and core-shear buckling (Ko and Jackson, 1993) depended on the shear mechanical properties of the core. Douville and Le Grognec (2013) found that in global buckling, the compression properties of the core had negligibly affected mechanical failure. Castanié et al. (2008) found that core crushing mainly depended on the compression properties of the core. Finally, skin separation and wrinkling depended on the mechanical properties of the glue, skin, and core and on the type of load supporting the sandwich-structured composite.

Despite the abundance of information available about the mechanical behaviour of cork core sandwiches under diverse loads and cork materials under compression loads, there is no information available regarding the behaviour of natural cork and its agglomerates under different loads. Additionally, little information is available about the mechanical properties of natural corks. Therefore, this study focused on these aspects by testing different cork agglomerates and natural cork sheets under pure compression, traction, and shear loads.

2. Materials

Six types of cork and cork agglomerates and high-density (60, 70, 80, and 100 kg/m^3) EPS (denoted by 'EPS' and the corresponding density) foams and their properties are listed in Table 1. These materials were studied for their potential application to mechanically high-demanding sandwich cores. EPS 70 was obtained in a 500 × 400 × 28-mm sheet; the others, in 100 × 100 × 28-mm sheets.

Three white cork (WC) agglomerates (usually called 'agglomerated cork'), natural cork (NC) material, black agglomerate (BA) cork (usually called 'expanded cork'), and brown agglomerate cork (AC) (Table 1) showing different grain sizes were used (Figure 1).

NC sheets are obtained from the bark of a cork-oak tree by means of axes and specially designed cutting machines used to remove only the external bark layer and produce regular, uniform, flat sheets, which dimensions vary depending on how the sheets are cut and the tree itself. The most common NC sheets are commercially available in lengths and widths [both] and thicknesses in ranges 100–600 and 3–15 mm, respectively.

Cork agglomerates are obtained after a more complex process in which recycled cork agglomerates and/or NC are mechanically chopped and sifted to obtain granules of different sizes, which are subsequently formed into bricks and/or regular sheets under heat and pressure and/or by mixing the granules with binders. The main advantages of agglomerates are that they have fewer dimensions and shape limitations. Therefore, agglomerated materials exhibit different mechanical properties depending on the binder used and the granule size.

WC agglomerates are manufactured using polyurethane (PU) binders and are heated between 110 and 150 °C. Although bio-degradable water-based glues are sometimes used, the most common binders are non-bio-degradable resins such as phenolic and vinyl resins, polyester, and epoxy. Hence, the resultant agglomerates are no longer completely renewable. As with regular agglomerates, the mechanical properties of WC agglomerates change depending on the granule size and, to a lesser extent, the resin used.

BAs are manufactured in high-temperature (300–370 °C) water steam under pressure (40 kPa) in an autoclave. The granules expand (hence the name 'expanded cork') and bind together owing to naturally exuded suberin resin.

In this study, the NC, 3 WC agglomerates prepared with different binders and densities, and 1 BA and 1 AC were obtained in 600 × 100 × 10-, 915 × 610 × 10-, and 1000 × 500 × 20-mm sheets, respectively.

Despite cork being a natural material, some cork agglomerates use non-renewable binders such as PU to join the grains. Although cork naturally generates its own binder, the naturally exuded suberin exhibits poor mechanical properties that negatively affect the behaviour of the whole material. Similarly, balsa wood is sealed using epoxy or polyester, both of which are petroleum-based binders.

3. Methods

The materials were studied under quasi-static traction and shear testing using an 8032 INSTRON® universal test machine operated at 5 mm/min for the tensile and compression tests and 0.50 mm/min for the shear test. At least 5 specimens of each material were tested, and the average test results were used for the analysis. All the

specimens were machined using a Roland MDX 20 CNC mill. Five specimens of each material were tested, and stress–strain and absorbed energy–strain curves were plotted for the average results. The maximum standard deviation for the main parameters was < 6.3% of the average values.

3.1. Compression test

The ASTM D1621 standard was followed to test the specimens. However, owing to the limitations of the original cork sheets, a 50 × 50-mm rectangular prism specimen was tested at the maximum thickness. This method is like that used in other EPS and cork-compression studies (Supplementary Figure 1).

The forces and displacements used to determine the stress–strain and absorbed energy–strain curves were obtained using the INSTRON® universal test machine. By comparing the results to the sample density, the specific stress–strain and absorbed energy–strain curves were obtained.

The EPS, cork, and cork agglomerates all generated similar stress–strain curves under the compression loads defined by the Ashbymodel developed by Gibson and Ashby (1997). Doroudiani and Kortschot (2003) indicated that the EPS stress–strain curve exhibited three well-defined density-dependent linear zones indicating linear elastic behaviour by the slope of the elastic Young's modulus of the material. Later, in the 'plateau zone', the cells began to collapse at an approximately constant rate. In this zone, the stress levels increase slowly, which defines the plateau of the Young's modulus. Finally, the densification zone appears where the opposing walls in the cells meet, causing the stress to increase steeply (Figure 2). The transition between the elastic and plateau zones was identified using Young's elastic modulus, which is the slope of the curve in the elastic zone. When the curve differs by more than 0.2%, a plateau zone

is reached. By the same method, the densification point was identified by the intersection point between the line defined by the slope of the plateau zone and a tangent curve in the densification zone, as obtained using either the bulk modulus of non-foaming EPS or the shape of the densification zone for cork agglomerates.

Fernandes et al. (2015) observed that although cork and its agglomerates exhibited similar stress–strain curves, the transition point between the elastic and plateau zones was not clearly defined. Furthermore, cork and its agglomerates usually present gentler and steeper slopes in the elastic and plateau zones, respectively, and elastically recover in the plateau zone and even in the densification zone, as demonstrated by Sanchez-Saez et al. (2015).

Owing to the shape of the stress–strain curves, the following main parameters (Figure 2) were obtained:

- $\sigma_{c,e}$: maximum tensile strength in elastic zone
- $\sigma_{cs,e}$: maximum specific tensile strength in elastic zone
- $\sigma_{c,d}$: maximum tensile strength at densification point
- $\sigma_{cs,d}$: maximum specific tensile strength at densification point
- $\varepsilon_{c,p}$: maximum elastic elongation
- $\varepsilon_{c,d}$: elongation at densification point
- E_c: elastic Young's modulus (slope of curve in elastic zone)
- E_p: plateau Young's modulus (slope of curve in plateau zone)

The total energy absorbed per unit volume of the material can be obtained from the following equation:

$$W = \int_{o}^{\varepsilon_i} \sigma d\varepsilon. \quad (1)$$

The total energy absorption can be decoupled into the following components:

Elastic energy absorption $W_e = \int_{o}^{\varepsilon_{c,p}} \sigma d\varepsilon.$ (2)

Energy absorbed in the plateau zone $W_p = \int_{\varepsilon_{c,p}}^{\varepsilon_{c,d}} \sigma d\varepsilon.$ (3)

The specific parameters are obtained by dividing the components by the material density (ρ) and are useful for comparing the mass properties of material samples instead of the volumetric properties. The parameters are as follows:

- E_{cs}: specific elastic Young's modulus
- E_{ps}: specific plateau Young's modulus
- W_{es}: specific elastic absorbed energy
- W_{ps}: specific energy absorbed in plateau zone

3.2. Tensile Test

The materials were tested using the ASTM D-638 standard for testing Type III specimens fabricated using a specific geometry to reduce the influence of grain size on the results (Supplementary Figure 2).

Owing to the shapes of the stress–strain curves, the following main parameters were obtained (Supplementary Figure 3):

- $\sigma_{t,max}$: tensile strength at break point (stress at failure point)
- $\varepsilon_{t,max}$: elongation at break point (failure point)
- E_t: yield strength under tensile load (slope of stress–strain curve)

By the same method used in the compression test, the specific properties are obtained by dividing the parameters by the material density (ρ) as follows:

- $\sigma_{ts,max}$: specific tensile strength at break point
- E_{ts}: specific elastic modulus under traction load

Chen et al. (2015) tested low-density EPS under traction and compression loads and found that the specimens exhibited linear elasticity with brittle failure. They used ASTM D-638-based specimen geometry to reduce the influence of discontinuities between the grains. Furthermore, Crouvisier-Urion et al. (2018) determined the main influence of the binders on the mechanical properties of cork agglomerate specimens prepared using ASTM D-638-based geometry and found that the materials exhibited linear elasticity with brittle failure.

3.3. Shear test

Because the specimens in the current study were tested following the ASTM 273 standard, we machined a 50 × 120 × 10-mm sheet firmly supported by two steel plates bonded using a structural epoxy adhesive. The plates were attached to two hinges that were geometrically designed and placed to ensure that the force line of action passed through the diagonally opposite corners of the composite. Under these experimental conditions, a test is invalid if there are adhesion or core-to-plate adhesive failures. Because the quantities of the EPS 60, 80, and 100 foams and their sheets were limited, it

was only possible to test the EPS 70 foams (Supplementary Figure 4).

The main properties obtained using the shear test are as follows (Supplementary Figure 5):

- Shear stress (τ) versus engineering shear strain (γ) response
- Specific shear stress (τ_s) versus engineering shear strain (γ) response
- τ_u Ultimate shear strength at point of maximum stress
- τ_{us}: Ultimate specific shear strength
- γ_u: Engineering shear strain at break point of maximum stress
- G: Shear chord modulus of elasticity (slope of stress–strain curve)
- G_s: Specific shear chord modulus of elasticity

Andersson et al. (2009) followed the ISO 1922 standard to test polyurethane rigid (PUR) foam under various shear loads and indicated that the mechanical properties were similar to those measured following the ASTM 273 standard. In addition, Canakci et al. (2016) and Canada (2018) both used a direct shear test to characterise low-density EPS and determined how the material density influenced the material rigidity. Furthermore, Ling et al. (2018a; 2018b) tested the static and dynamic behaviours of EPS under combined shear and compression loads.

Although some studies have been conducted on EPS and cork under shear loads to analyse the behaviour of sandwich panels fabricated with skins, no such tests have been conducted on skinless panels using only the core.

4. Results and discussion

4.1. Compression test results

Although no specific standard is available for testing EPS foams or cork agglomerates, the ISO 844, ASTM D1621, and ASTM 3574 standards could be applied because EPS is a rigid cellular plastic, and cork agglomerates exhibit similar properties. According to the ASTM 3574, ASTM D1621, and ISO 844 standards, the preferred specimens are 50 × 50 × 25-mm prisms; the minimum specimen dimensions are 25.4 × 25.4 × 25.4 mm; and although the minimum thickness is 50 mm, the preferred specimens are 50 × 100 × 100-mm prisms; respectively. For analysing sandwich cores, the ASTM C365 standard requires a circular or square cross-section specimen where the minimum cross-section depends on the material. Owing to the limited thickness of some of the materials, the test specimens were adapted to a prismatic shape exhibiting a box cross-section of 50 × 50-mm at the maximum thickness. Because all the other aspects of the standards are similar, the ASTM D1621 standard was used but instead with the maximum thickness of the original sheet plates.

The stress–strain curves obtained for all the compressed materials presented the typical behaviour of a foam exhibiting elastic, plateau, and densification zones according to the model developed by Gibson and Ashby (1997) and as indicated by Silva et al. (2005). The NC exhibited gentler and steeper slopes in the elastic and plateau zones, respectively. Lakreb et al. (2015) and Silva et al. (2005) both obtained similar stress–strain curves from similar parameters.

Figure 3 and Supplementary Table 1 show that the NC exhibited the highest stiffness of all the cork products and that although the stress–strain curve exhibited a shape similar to that obtained for the EPS, it exhibited a linearly increasing plateau zone instead of a

flat one and an exponentially increasing densification zone. All the other corks and agglomerates exhibited similar stress–strain curves. The materials exhibited a shallower elastic zone and a gentler transition to the plateau zone. Because the stress–strain curves obtained for the EPS foams exhibited a flat plateau zone (which implies both constant energy-absorption capability [Figure 4] and stiffness), the cork agglomerates clearly exhibited both increased energy-absorption capability (Figure 4) and stiffness. However, the EPS 100 exhibited a higher elastic modulus but a lower strength in the elastic zone and at the densification point. The shape of the EPS stress–strain curves implies that the EPS foams all exhibited higher strengths in the elastic zone but similar ones at the densification point; however, the cork products densified earlier.

Compared to the other materials, although the balsa wood presented a similar elastic modulus, it did not follow the Ashby-Gibson model and instead exhibited an elastic behaviour with a much higher strength in the elastic zone, which makes balsa wood especially effective at supporting compression forces. Consequently, under compression, cork products cannot be substituted for balsa wood.

Additionally, the corks and their agglomerates densified with fewer deformations.

Among the cork agglomerates, the AC properties were like the WC 300 ones. In addition, the properties of all the WCs except for WC 275 improved with increasing density. The WC 275 exhibited the highest strength at the densification point, while the BA exhibited the lowest strength and stiffness. Furthermore, higher WC density clearly was associated with higher the strength and stiffness. It should be noted that although AC exhibited low density, it exhibited high strength and stiffness. Finally, the expanded BA exhibited the lowest strength and stiffness. Another important result shown in Figure 4 is that the lower density implies that both the EPS and cork agglomerates

densified later.

(Figure 3 [right]) compares the specific mechanical properties. Clearly, the EPS exhibited higher specific strength and stiffness, which were directly dependent on the low density, in the densification and plateau zones.

Compared with cork and its agglomerates, the NC and AC exhibited mid-range specific strengths and stiffnesses. The other materials exhibited similar specific mechanical properties; therefore, the lower-density materials clearly densified later mainly because more air was trapped inside them. Consequently, higher deformations were necessary to expel the trapped air.

Although the NC absorbed more energy (Figures 4 and 5) than the other materials, the specific energy of all the EPS foams was higher. Because of the shape of the stress–strain curves obtained for the cork agglomerates, although initially the agglomerates could absorb less energy, they absorbed more energy with increasing deformation and ultimately exhibited a higher energy-absorption capability than some of the EPS foams. Furthermore, all the higher-density WCs except for WC 275 clearly exhibited higher energy-absorption capability. The WC 275, on the other hand, exhibited low strain and a slightly higher energy-absorption capability. Finally, the BA exhibited the lowest energy absorption capability.

The cork products exhibited lower energy-absorption capabilities per unit weight, while the NC exhibited the highest quasi-linear energy-absorption capability among the cork products. The AC exhibited the second-highest energy-absorption capability per unit weight. Furthermore the WC and BA clearly exhibited similar energy-absorption capabilities per unit weight.

4.2. Tensile test results

Despite the specific standards for analysing sandwich cores under tensile loads, standards such as ASTM C297 cannot be used to characterise EPS or cork materials. Additionally, no specific standard is available for testing EPS foams, cork and its agglomerates, or rigid cellular plastics under tensile loads. However, because all these materials exhibit similar behaviours, Doroudiani (2003) tested them according to the ASRM D-638 standard. Although the ASTM D3574–17 and ASTM D1623 -17 standards could also be used to test such materials, the ASTM D1623 -17 standard requires the use of cylindrical specimens, which could not be prepared using cork sheets. Therefore, the ASTM D1623 -17 standard was not used in this study. The main differences between the other standards are the test-specimen thickness (which is variable for the first standard and fixed to 12.5 for the second one), the main geometric dimensions of the specimen, and the methods used to prepare the specimens. In this study, owing to the limited thickness of the NC and some cork-agglomerate sheets, the ASTM D-638 standard for Type-III specimens was used. Additionally, some materials are comprised of large grains (i.e., EPS 100 and BA 100 grains are between 2 and 3 mm and 4 and 10 mm, respectively).

Consequently, the small thicknesses and widths of the narrow specimen portions imply that the grain size could distort the results. In addition, some EPS sheets are limited by their geometry. Hence, all the specimens were machined and tested based on their maximum thickness to reduce the influence of the grain size, and a modified type-III-specimen-based geometry was proposed (Supplementary Figure 2), which enabled all the materials to be used and exhibited a width of at least three times larger than the largest grains in BA 100 and six-or-more times larger than the largest grains in the other materials. Additionally, an extensometer was used to determine the distance between

the two specific points used to measure the strain.

Although the materials could be tested following the standard ISO 1926: Rigid cellular plastics—Determination of tensile properties, which uses a similar bone-like geometry but with a thickness of 4 mm, the grains in the materials are still larger than that. Therefore, the ISO 1926 standard was not used.

The stress–strain curves obtained for all the materials exhibited linear elasticity and brittle failure (Figure 6 [left]), as previously described by both Lakreb et al. (2015) and Silva et al. (2005), who found brittle failure similar to that depicted in Figure 7. The mechanical properties and stress–strain curves (Supplementary Table 2 and Figure 6 [left]) also showed similarities to those in these studies. From the results shown in Figure 6 [left], Figure 8 [left], and Supplementary Table 2, the NC exhibited the highest tensile strength, approximately twice that of the second-strongest EPS foam at the break point, despite showing similar yield strengths. Additionally, the NC reached a higher deformation than the EPS. Among the specific mechanical properties (Figure 6 [right] and Figure 8 [right]), the EPS exhibited the highest specific and yield strengths owing to the high density of the NC and the low density of the EPS.

Although all the WC specimens exhibited lower rigidities and reached higher deformations than the EPS specimens, the former could only support lower loads. However, there was no clear relationship between the density and mechanical properties of these materials.

These results were attributed to the internal structure of the binder joining together the agglomerate grains. The NC structure consists of joined cellules. Consequently, this natural structure exhibits higher strength, especially under tensile loads, than that of a structure consisting of chopped granules joined together using binders. Similarly,, the

EPS foam structure is not joined. Among the binders used to prepare the agglomerates in this study, the epoxy binders exhibited higher strength than the natural suberin; therefore, WC and BA exhibited reduced strength under tensile loads. Additionally, these materials exhibited the largest grains, which generated gaps in the transverse area of the specimens, thereby further weakening the strength.

Among the specific mechanical properties, all the EPS and NC specimens exhibited similarly high maximum specific and yield strengths compared to the very low-strength agglomerates.

4.3. Shear test results

Depending on the range of applications, materials can be tested using various shear tests including direct shear tests for geotechnical applications; Iosipescu tests (defined in the ASTM-D 7078 and ASTM-D 5379 standards) for composites and determining the influence of fibre orientation on shear strength; and 2-and 3-point bending tests (ASTM C393) for composites and their skins. This study used the ASTM 273 standard, which measures the shear properties of sandwich cores to determine the shear strength parallel to the plane of sandwich-structured composites.

Although the shear properties of cores could be tested following other standards such as the ISO 1922 standard (which requires a 250 × 50 × 25-mm specimen), they were not used in this study because the thickness of some of the materials was limited (Figure 4 of the Supplementary material).

The analysis results shown in Figure 9 [left] and Figure 10 [left] and Supplementary Table 3 clearly show that, except for the BA, all the other materials exhibited higher strengths than the EPS. In addition, most of them could support larger deformation

before reaching the break point and as a result, exhibited a lower shear modulus. The NC was the strongest material, and the AC was the second strongest. The WC did not exhibit any clear relationship between density and the mechanical properties, and the BA was the weakest material. These findings are consistent with the stress–strain curves and mechanical properties previously reported by Lakreb et al. (2015), Reis and Silva (2009), and Sadeghian et al. (2018).

The specific mechanical properties are shown in Figure 9 [right] and Figure 10 [right]. Because the EPS exhibited the lowest density, this material exhibited the highest specific shear strength followed by the NC. Because the BA exhibited the second-lowest density, it exhibited mid-range specific shear strength. Some of the WCs exhibited the lowest specific strength owing to their mid-range mechanical properties and high densities.

As shown in Figure 11, all the specimens exhibited similar internal core failures, which is representative of such materials (Lakreb et al., 2015; Reis and Silva, 2009; Sadeghian et al., 2018). The failure initially appeared in the diagonal area of the specimen in different zones and progressed until reaching catastrophic failure. Initially, the material exhibited a predominantly elastic regime; however, after a relatively low strain, some zones inside the diagonal began to fail. In the second stage, some additional failures appeared in the same diagonal at the specimen edges. Subsequently, existing cracks propagated and more cracks nucleated and propagated along the specimen and converged to a few main cracks prior to total failure.

5. Conclusions

This article describes the mechanical characterisation of different cork agglomerates and NC under simple loads required for selecting the correct material for specific

applications. These data could be useful for not only designing cores in sandwich-structured composites but also other applications such as the use of cork in helmet liners or sports equipment.

The main study findings were as follows:

Cork and its agglomerates exhibited considerably reduced mechanical properties compared with balsa wood under all loads.

The stress–strain curves obtained for the compressed NC and cork agglomerates exhibited a shallow elastic zone and an increasing plateau zone instead of a flat one. Consequently, the materials exhibited constantly increasing rather than constant energy absorption except for the NC, which stress–strain curve exhibited a shape typical of the stress–strain curve obtained for the EPS foam. Additionally, the NC exhibited the highest mechanical properties, and the other agglomerates exhibited high mechanical properties under high strain. As a result, these materials supported higher compression loads before reaching global buckling or core-crushing failure. However, the EPS foam exhibited higher specific mechanical properties. In addition, all the agglomerates exhibited similar specific stress–strain curves and mechanical properties.

From the tensile properties, although the cork agglomerates reached higher deformations, they exhibited lower strengths. Furthermore, the tensile properties were notably lower for both the BA and AC because of the specific binder and grain size, which reduced the effective area under traction loads. The NC exhibited the highest strength and low stiffness. However, the EPS exhibited a higher specific strength.

Under shear loads, the NC exhibited the highest shear strength and the other cork agglomerates exhibited higher shear strength than the EPS 70; therefore, they could

support higher loads. Consequently, core-shear failure and buckling occurred under higher loads. Nevertheless, the EPS 70 exhibited the highest specific shear strength.

The NC exhibited considerably higher mechanical and specific properties than the other cork products under all loads and exhibited higher strength and stiffness than the EPS and similar specific properties. Therefore, NC is a perfect substitute for these materials. However, because NC is natural, its dimensions are somewhat limited. To solve this problem, multiple sheets of NC could be stacked, glued, and machined to obtain the desired thickness and dimensions.

Finally, owing to the absence of specific standards for testing cork products, the ASTM D1621, ASTM D-638, and ASTM 273 standards were adopted for the compression, tensile, and shear tests, respectively.

Author contribution: All the authors have accepted responsibility for the entire content of this submitted manuscript and approved submission.

Research funding: This work was supported by the "Ibercaja Foundation" young Research Grant. IberDoD HBCU/MI Basic Research Grant (grant number JIUZ-2018-TEC-09), the University of Zaragoza (Spain) and the research group ID-ERGO.

Conflict of interest statement: The authors declare no conflicts of interest

References

American Society for Testing and Materials 2020, *Standard Test Method for Shear Properties of Sandwich Core Material,* ASTM C273 / C273M - 20:2020, American Society for Testing and Materials, West Conshohocken.

American Society for Testing and Materials 2016, *Standard Test Method for Flatwise Tensile Strength of Sandwich Constructions*, ASTM C297 / C297M – 16:2016, American Society for Testing and Materials, West Conshohocken

American Society for Testing and Materials 2020, *Standard Test Method for Core Shear Properties of Sandwich Constructions by Beam Flexurethod,* ASTM C393 / C393M - 20:2020, American Society for Testing and Materials, West Conshohocken.

American Society for Testing and Materials 2014, *Standard Test Method for Tensile Properties of Plastics,* ASTM D638 - 14:2014, American Society for Testing and Materials, West Conshohocken.

American Society for Testing and Materials 2016, *Standard Test Method for Compressive Properties of Rigid Cellular Plas*tics, ASTM D1621 – 16:2016, American Society for Testing and Materials, West Conshohocken.

American Society for Testing and Materials 2017, *Standard Test Method for Tensile and Tensile Adhesion Properties of Rigid Cellular Plastics,* ASTM D1623 - 17:2017, American Society for Testing and Materials, West Conshohocken.

American Society for Testing and Materials 2017, *Standard Test Methods for Flexible Cellular Materials—Slab, Bonded, and Molded Urethane Foams,* ASTM D3574 – 17:2017, American Society for Testing and Materials, West Conshohocken.

American Society for Testing and Materials 2019, *Standard Test Method for Shear Properties of Composite Materials by the V-Notched Beam Method ASTM D5379 / D5379M - 19e1*:2019, American Society for Testing and Materials, West Conshohocken

American Society for Testing and Materials 2020, *Standard Test Method for Shear Properties of Composite Materials by V-Notched Rail Shear Method,* ASTM D7078 / D7078M - 20e1:2020, American Society for Testing and Materials, West Conshohocken.

Andersson, A., Lundmark, S., Magnusson, A., Maurer, F.H.J., 2009. Shear behavior of flexible polyurethane foams under uniaxial compression. J. Appl. Polym. Sci. 111, 2290–2298. https://doi.org/10.1002/app.29244

Bach, M.R., Chalivendra, V.B., Alves, C., Depina, E., 2017. Mechanical characterization of natural biodegradable sandwich materials. Jnl of Sandwich Structures & Materials 19, 482–496. https://doi.org/10.1177/1099636215622143

Canakci, H., Alak, D., Celik, F., 2016. Evaluation of Shear Strength Properties of Modified Expanded Polystyrene Aggregate. Procedia Engineering 161, 606–610. https://doi.org/10.1016/j.proeng.2016.08.708

Carlsson, L.A., Sendlein, L.S., Merry, S.L., 1991. Characterization of Face Sheet/Core Shear Fracture of Composite Sandwich Beams. Journal of Composite Materials 25, 101–116. https://doi.org/10.1177/002199839102500105

Castanié, B., Aminanda, Y., Bouvet, C., Barrau, J.-J., 2008. Core crush criterion to determine the strength of sandwich composite structures subjected to compression after impact. Composite Structures 86, 243–250. https://doi.org/10.1016/j.compstruct.2008.03.032

Chen, W., Hao, H., Hughes, D., Shi, Y., Cui, J., Li, Z.-X., 2015. Static and dynamic mechanical properties of expanded polystyrene. Materials & Design 69, 170–180. https://doi.org/10.1016/j.matdes.2014.12.024

Crouvisier-Urion, K., Bellat, J.-P., Gougeon, R.D., Karbowiak, T., 2018. Mechanical properties of agglomerated cork stoppers for sparkling wines: Influence of adhesive and cork particle size. Composite Structures 203, 789–796. https://doi.org/10.1016/j.compstruct.2018.06.116

Díaz-Parralejo, A., Cuerda-Correa, E.M., Macías-García, A., Sánchez-González, J., Díaz-Díez, M.Á., 2014. The Excellent Mechanical Properties of Cork: A Novel Approach through the Analysis of Contact Stress. ISRN Materials Science 2014, 1–6. https://doi.org/10.1155/2014/898439

Doroudiani, S., Kortschot, M.T., 2003. Polystyrene foams. III. Structure-tensile properties relationships. J. Appl. Polym. Sci. 90, 1427–1434. https://doi.org/10.1002/app.12806

Douville, M.-A., Le Grognec, P., 2013. Exact analytical solutions for the local and global buckling of sandwich beam-columns under various loadings. International Journal of Solids and Structures 50, 2597–2609. https://doi.org/10.1016/j.ijsolstr.2013.04.013

Fernandes, F.A.O., Jardin, R.T., Pereira, A.B., Alves de Sousa, R.J., 2015. Comparing the mechanical performance of synthetic and natural cellular materials. Materials & Design 82, 335–341. https://doi.org/10.1016/j.matdes.2015.06.004

Gibson, L.J., Ashby, M.F., 1997. Cellular Solids: Structure and Properties, 2nd ed. Cambridge University Press. https://doi.org/10.1017/CBO9781139878326

Jardin, R.T., Fernandes, F.A.O., Pereira, A.B., Alves de Sousa, R.J., 2015. Static and dynamic mechanical response of different cork agglomerates. Materials & Design 68, 121–126. https://doi.org/10.1016/j.matdes.2014.12.016

Ko, W.L., Jackson, R.H., 1993. Compressive and shear buckling analysis of metal matrix composite sandwich panels under different thermal environments. Composite Structures 25, 227–239. https://doi.org/10.1016/0263-8223(93)90169-Q

Lakreb, N., Bezzazi, B., Pereira, H., 2015. Mechanical behavior of multilayered sandwich panels of wood veneer and a core of cork agglomerates. Materials & Design (1980-2015) 65, 627–636. https://doi.org/10.1016/j.matdes.2014.09.059

Laura, P.A.A., Rossit, C.A., 2001. The Behavior of Sandwich Structures of Isotropic and Composite Materials. Ocean Engineering 28, 1437–1438. https://doi.org/10.1016/S0029-8018(01)00013-0

Le Duigou, A., Deux, J.-M., Davies, P., Baley, C., 2011. PLLA/Flax Mat/Balsa Bio-Sandwich Manufacture and Mechanical Properties. Appl Compos Mater 18, 421–438. https://doi.org/10.1007/s10443-010-9173-8

Ling, C., Ivens, J., Cardiff, P., Gilchrist, M.D., 2018a. Deformation response of EPS foam under combined compression-shear loading. Part I: Experimental design and quasi-static tests. International Journal of Mechanical Sciences 144, 480–489. https://doi.org/10.1016/j.ijmecsci.2018.06.014

Ling, C., Ivens, J., Cardiff, P., Gilchrist, M.D., 2018b. Deformation response of EPS foam under combined compression-shear loading. Part II: High strain rate dynamic tests. International Journal of Mechanical Sciences 145, 9–23. https://doi.org/10.1016/j.ijmecsci.2018.06.015

Najafi, M., Darvizeh, A., Ansari, R., 2020. Characterization of moisture effects on novel agglomerated cork core sandwich composites with fiber metal laminate facesheets. Jnl of Sandwich Structures & Materials 22, 1709–1742. https://doi.org/10.1177/1099636218789613

Reis, L., Silva, A., 2009. Mechanical Behavior of Sandwich Structures using Natural Cork Agglomerates as Core Materials. Jnl of Sandwich Structures & Materials 11, 487–500. https://doi.org/10.1177/1099636209104523

Sadeghian, P., Hristozov, D., Wroblewski, L., 2018. Experimental and analytical behavior of sandwich composite beams: Comparison of natural and synthetic materials. Jnl of Sandwich Structures & Materials 20, 287–307. https://doi.org/10.1177/1099636216649891

Sanchez-Saez, S., Barbero, E., Garcia-Castillo, S.K., Ivañez, I., Cirne, J., 2015. Experimental response of agglomerated cork under multi-impact loads. Materials Letters 160, 327–330. https://doi.org/10.1016/j.matlet.2015.08.012

Silva, S.P., Sabino, M.A., Fernandes, E.M., Correlo, V.M., Boesel, L.F., Reis, R.L., 2005. Cork: properties, capabilities and applications. International Materials Reviews 50, 345–365. https://doi.org/10.1179/174328005X41168

Triantafillou, T.C., Gibson, L.J., 1987. Failure mode maps for foam core sandwich beams. Materials Science and Engineering 95, 37–53. https://doi.org/10.1016/0025-5416(87)90496-4

Wadsworth, D.J., Horrigan, D.P.W., Moltschaniwskyj, G., Collins, I., 2009. Facesheet Wrinkling of Damaged Honeycomb Sandwich Structures. Jnl of Sandwich Structures & Materials 11, 105–131. https://doi.org/10.1177/1099636209103555

Zaini, E., Azaman, M., Jamali, M., Ismail, K., 2020. Synthesis and characterization of natural fiber reinforced polymer composites as core for honeycomb core structure: A review. Jnl of Sandwich Structures & Materials 22, 525–550. https://doi.org/10.1177/1099636218758589

Table 1. Studied materials, their density and their grain size.

Figure 1. Cork and cork agglomerates studied.

Figure 2. Typical stress-strain curve for the EPS under compression efforts.

Figure 3. Left: stress-strain curve for EPS and cork and cork products under compression efforts; right: specific stress-strain curve for EPS and cork and cork products under compression efforts.

Figure 4. Left: energy-strain curve for EPS and cork and cork products under compression efforts; right: specific energy-strain curve for EPS and cork and cork products under compression efforts.

Figure 5. Left: absorbed energy per unit of volume until densification point; right: absorbed energy per unit of weight until densification point.

Figure 6. Left: stress-strain curve for EPS and cork and cork products under tensile efforts; right: specific stress-strain curve for EPS and cork and cork products under tensile loads.

Figure 7. Brittle failure of the WC275.

Figure 8. Left: tensile strength at break point under tensile effort; right: specific tensile strength at break point under tensile effort.

Figure 9. Left: shear stress-strain curve for EPS and cork and cork products under shear loads; right: specific shear stress-strain curve for EPS and cork and cork products under shear loads.

Figure 10. Left: ultimate shear strength at point of maximum stress; right: ultimate specific shear strength at point of maximum stress.

Figure 11. Evolution of the failure in the shear test: (a): initial point, (b) elastic domain, (c) beginning of failure inside the cork agglomerate, (d) beginning of failure in the

edges of the cork agglomerate, (e-h) several crack propagating and initiating, (i) final failure.

Supplementary Figure 1. Left: Geometry of the compression specimens (dimensions in mm). Right: compression test of the EPS 100

Supplementary Figure 2. Left: Geometry of the traction specimens (dimensions in mm). Center: traction test of the EPS 80. Right: traction test of the WA275

Supplementary Figure 3. Typical stress-strain curve for brittle materials (like EPS) under traction efforts.

Supplementary Figure 4. Left: Geometry of the traction specimens (dimensions in mm). Right: shear test of the WA275

Supplementary Figure 5. Typical stress-strain curve for like EPS under shear efforts.

Supplementary Table 1. Mechanical properties of the studied materials under compression efforts

Supplementary Table 2. Main mechanical properties of EPS, cork and cork products under tensile loads

Supplementary Table 3. Main mechanical properties of EPS, cork and cork products under ASTM 273 shear loads

Figure 1. Cork and cork agglomerates studied.

233x145mm (120 x 120 DPI)

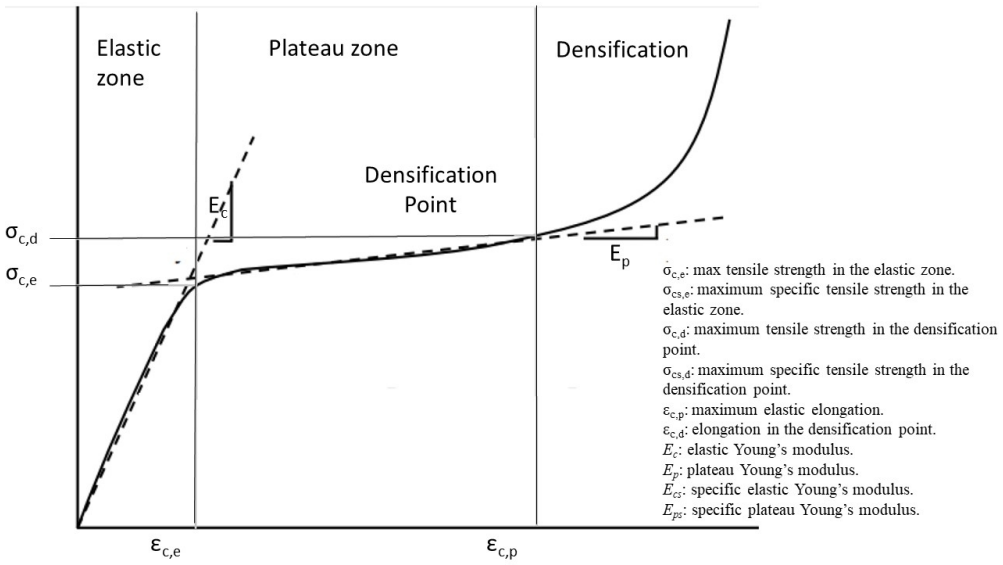

Figure 2. Typical stress-strain curve for the EPS

338x190mm (96 x 96 DPI)

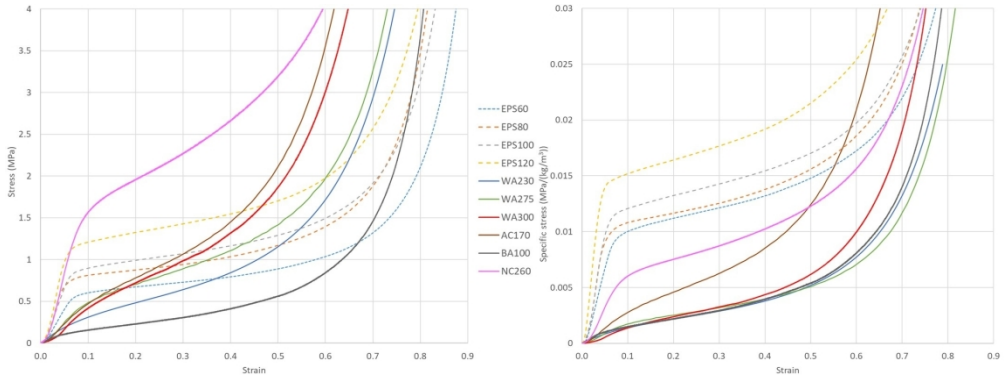

Figure 3. Left: stress-strain curve for EPS and cork and cork products under compression efforts; right: specific stress-strain curve for EPS and cork and cork products under compression efforts.

566x210mm (96 x 96 DPI)

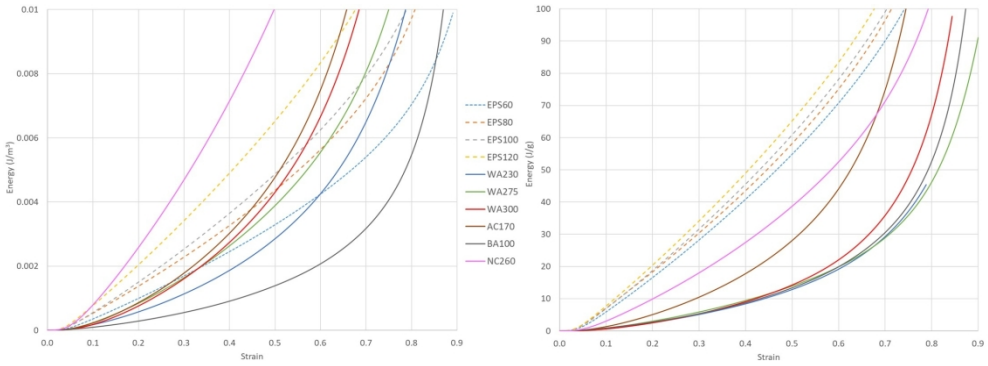

Figure 4. Left: energy-strain curve for EPS and cork and cork products under compression efforts; right: specific energy-strain curve for EPS and cork and cork products under compression efforts.

590x210mm (96 x 96 DPI)

Figure 5. Left: absorbed energy per unit of volume until densification point; right: absorbed energy per unit of weight until densification point

590x210mm (96 x 96 DPI)

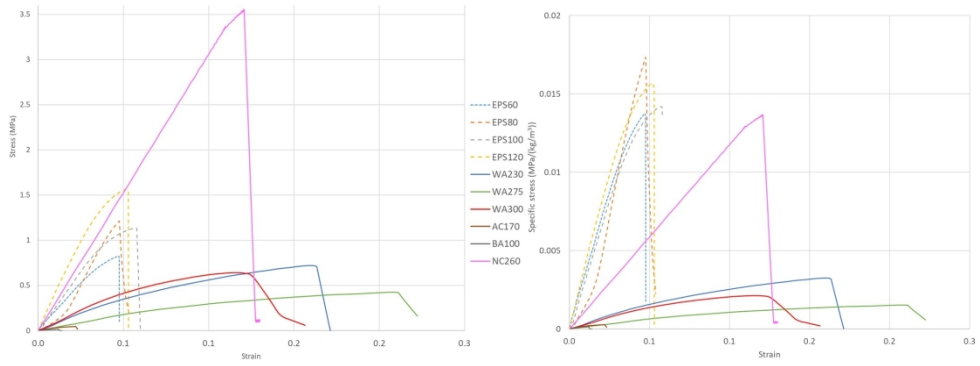

Figure 6. Left: stress-strain curve for EPS and cork and cork products under tensile efforts; right: specific stress-strain curve for EPS and cork and cork products under tensile loads.

590x210mm (96 x 96 DPI)

Figure 7. Brittle failure of the WC275.

113x155mm (120 x 120 DPI)

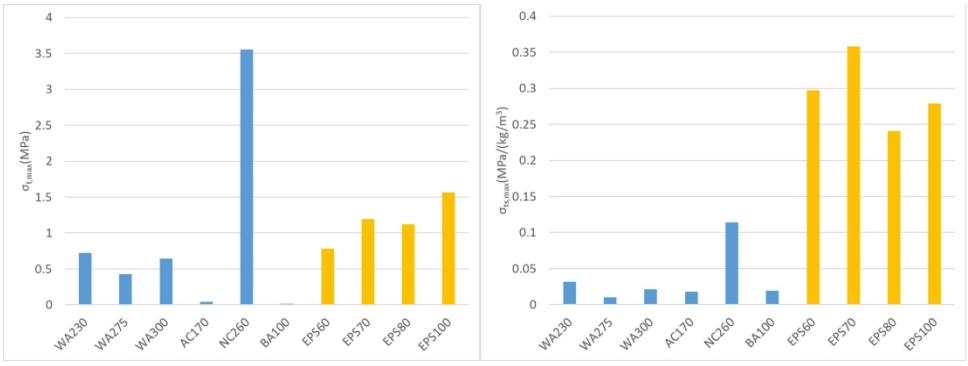

Figure 8. Left: tensile strength at break point under tensile effort; right: specific tensile strength at break point under tensile effort.

590x210mm (96 x 96 DPI)

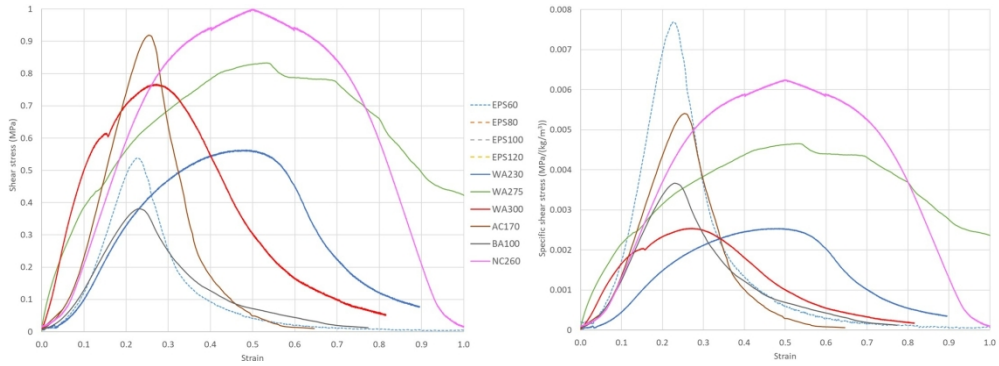

Figure 9. Left: shear stress-strain curve for EPS and cork and cork products under shear loads; right: specific shear stress-strain curve for EPS and cork and cork products under shear loads.

590x210mm (96 x 96 DPI)

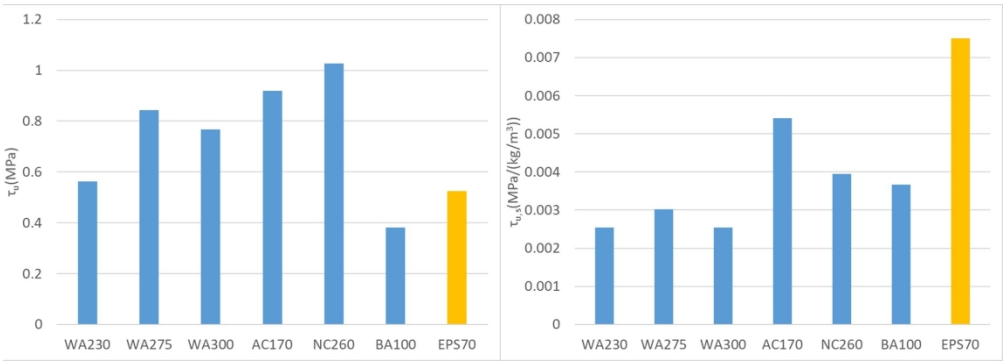

Figure 10. Left: ultimate shear strength at point of maximum stress; right: ultimate specific shear strength at point of maximum stress

590x210mm (96 x 96 DPI)

Figure 11. Evolution of the failure in the shear test: (a): initial point, (b) elastic domain, (c) beginning of failure inside the cork agglomerate, (d) beginning of failure in the edges of the cork agglomerate, (e-h) several crack propagating and initiating, (i) final failure.

274x157mm (120 x 120 DPI)

	Type	Designated density (kg/m^3)	Actual Density (kg/m^3)	Grain size (mm)	Thickness (mm)	Binder	Moisture content (%)
EPS60	Exp. Polystyrene	60	64.8	2.5	28	N/A	
EPS70	Exp. Polystyrene	70	71.1	2.3	28	N/A	
EPS80	Exp.Polystyrene	80	80.7	2.15	28	N/A	
EPS100	Exp.Polystyrene	100	100.9	1.95	28	N/A	
WA300	White agglom.	300	302	2-5	10	PU	5.8
WA275	White agglom.	275	279	0.5-2	10	PU	6.1
WA230	White agglom.	230	222	1-3	10	PU	6.4
AC170	Cork agglomerate	170	172	2-5	20	PU	6.7
BA100	Black agglomerate	100	104	4-10	20	Suberin	6.8
NC260	Natural cork	260	263	N/A	10	None	5.3
UL BC	Ultra lite balsa wood	100	N/A	N/A	N/A	N/A	7.0
WG BC	Wind grade balsa wood	132	N/A	N/A	N/A	N/A	6.7
SG BC	Standard grade balsa wood	152	N/A	N/A	N/A	N/A	6.2
FH BC	Heavy weight balsa wood	280	N/A	N/A	N/A	N/A	5.8

Table 1. Studied materials, their density, their grain size and moisture content.

Mat.	E_c	E_p	$\sigma_{c.e}$	$\sigma_{c.d}$	$\varepsilon_{c.p}$	$\varepsilon_{c.d}$	E_{cs}	E_{ps}	$\sigma_{cs.d}$	$\sigma_{cs.e}$	W_e	W_p	W_{es}	W_{ps}
Units	MPa				%		(MPa/kg/m^3)				J/m^3		J/kg	
WA230	4.42	2.00	0.23	1.07	5.2	47.2	0.019	0.0087	0.0010	0.0047	5.98E-05	0.0027	2.6E-07	1.2E-05
WA275	3.93	2.40	0.53	1.44	13.5	51.4	0.014	0.0087	0.0019	0.0052	0.000358	0.0042	1.3E-06	1.5E-05
WA300	3.94	2.95	0.52	1.38	13.2	42.4	0.013	0.0098	0.0017	0.0046	0.000343	0.0028	1.1E-06	9.3E-06
AC170	4.17	3.54	0.43	1.42	10.3	38.3	0.025	0.0208	0.0025	0.0084	0.000221	0.0026	1.4E-06	1.6E-05
NC260	16.05	3.68	1.53	2.78	9.53	43.5	0.062	0.0142	0.0059	0.0107	0.000729	0.0072	2.8E-06	2.8E-05
BA100	7.92	0.98	0.19	0.63	2.4	47.2	0.079	0.0098	0.0019	0.0063	2.28E-05	0.0012	2.3E-07	1.2E-05
EPS60	9.81	1.20	0.51	1.22	5.2	64.6	0.163	0.0199	0.0085	0.0203	0.000133	0.0046	2.2E-06	7.7E-05
EPS70	19.19	1.18	0.71	1.37	3.7	59.7	0.274	0.0168	0.0101	0.0196	0.000131	0.0057	1.9E-06	8.1E-05
EPS80	15.73	1.20	0.78	1.41	4.96	57.6	0.197	0.0150	0.0098	0.0176	0.000193	0.0056	2.4E-06	0.00007
EPS100	21.00	1.24	1.18	1.76	5.62	52.3	0.210	0.0124	0.0118	0.0176	0.000332	0.0066	3.3E-06	6.6E-05
ULBC	7.5	N/A	2238	N/A	N/A	N/A	0.08	N/A	22.38	N/A	N/A	N/A	N/A	N/A
WG BC	12.5	N/A	3100	N/A	N/A	N/A	0.09	N/A	23.48	N/A	N/A	N/A	N/A	N/A
SG BC	14.4	N/A	3574	N/A	N/A	N/A	0.09	N/A	23.51	N/A	N/A	N/A	N/A	N/A
HW BC	21.6	N/A	5690	N/A	N/A	N/A	0.08	N/A	21.88	N/A	N/A	N/A	N/A	N/A

Table 2. Mechanical properties of the studied materials under compression efforts

Mat.	G	τ_u	G_s	τ_{us}	γ_u
Units	MPa		MPa/kg/m^3		%
WA230	1.65	0.563	0.00743	0.00254	0.251
WA275	1.53	0.843	0.00548	0.00302	0.569
WA300	3.46	0.767	0.01146	0.00254	0.559
AC170	3.94	0.919	0.02318	0.00541	0.262
NC260	3.137	1.026	0.01207	0.00395	0.487
BA100	1.86	0.381	0.01788	0.00366	0.239
ESP70	4.97	0.525	0.07100	0.00750	0.232
UL BC	110	1.88	N/A	1.1	0.0188
WG BC	162	2.36	N/A	1.22	0.0178
SG BC	186	2.72	N/A	1.22	0.0178
FH BC	364	5.57	N/A	1.3	0.0198

Table 4. Main mechanical properties of EPS, cork and cork products under ASTM 273 shear loads

ELSEVIER

Certificate of Elsevier Language Editing Services

The following article was edited by Elsevier Language Editing Services:

"Experimental study of natural cork and cork agglomerates as a substitute for high-density eps foams in sandwich cores."

Authored by:

Ramon Miralbes Buil

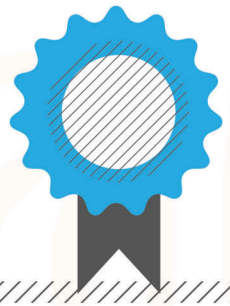

Date: 22-Apr-2021

Serial number: LE-210469-DF0AD074D1CA

https://mc.manuscriptcentral.com/holz